Received: 4 October 2023 | Revised: 18 December 2023 | Accepted: 19 December 2023

DOI: 10.1002/pmic.202300384

DATASET BRIEF

Proteomics
Proteomics and Systems Biology

Proteome profile of the cerebellum from α7 nicotinic acetylcholine receptor deficient mice

Karolina Magdalena Caban[1] | Pia Seßenhausen[2] | Jan Bernard Stöckl[1] | Bastian Popper[3] | Artur Mayerhofer[2] | Thomas Fröhlich[1]

[1]Laboratory for Functional Genome Analysis LAFUGA, Gene Center, LMU München, München, Germany

[2]Biomedical Center Munich (BMC), Cell Biology, Anatomy III, Faculty of Medicine, Ludwig Maximilian University of Munich, Planegg-Martinsried, Germany

[3]Biomedical Center (BMC), Core Facility Animal Models, Faculty of Medicine, Ludwig-Maximilians-University Munich, Planegg-Martinsried, Germany

Correspondence
Thomas Fröhlich, Feodor-Lynen-Str. 25, München 81377, Germany.
Email: frohlich@genzentrum.lmu.de

Artur Mayerhofer and Thomas Fröhlich are joint senior authors.

Funding information
Deutsche Forschungsgemeinschaft, Grant/Award Number: 432434245

Abstract

The alpha7 nicotinic acetylcholine receptor (α7 nAChR; *CHRNA7*) is expressed in the nervous system and in non-neuronal tissues. Within the central nervous system, it is involved in various cognitive and sensory processes such as learning, attention, and memory. It is also expressed in the cerebellum, where its roles are; however, not as well understood as in the other brain regions. To investigate the consequences of absence of CHRNA7 on the cerebellum proteome, we performed a quantitative nano-LC-MS/MS analysis of samples from CHRNA7 knockout (KO) mice and corresponding wild type (WT) controls. Liver, an organ which does not express this receptor, was analyzed, in comparison. While the liver proteome remained relatively unaltered (three proteins more abundant in KOs), 90 more and 20 less abundant proteins were detected in the cerebellum proteome of the KO mice. The gene ontology analysis of the differentially abundant proteins indicates that the absence of CHRNA7 leads to alterations in the glutamatergic system and myelin sheath in the cerebellum. In conclusion, our dataset provides new insights in the role of CHRNA7 in the cerebellum, which may serve as a basis for future in depth-investigations.

KEYWORDS
acetylcholine, cerebellum, mass spectrometry, nicotinic receptor

Nicotinic acetylcholine receptors (nAChRs) are a diverse family of ligand-gated ion channels that are composed of five subunits which assemble symmetrically around an axis perpendicular to the plasma membrane [1]. They are well known to mediate neurotransmission in the nervous systems in response to the neurotransmitter acetylcholine [2]. There are twelve neuronal-type nAChR subunits in this family (α2–α10 and β2–β4). Localization, physiological, and pharmacological properties of each receptor subtype are determined by the subunit composition [3]. In α7 nAChRs, the α7 subunits, encoded by the *Chrna7* gene [4], form a homopentamer with a high permeability for calcium ions [5]. Recent studies indicated that α7 together with β2 subunits can also form heteromeric α7β2 nAChRs [6]. These receptors have altered ion selectivity, gating kinetics, and sensitivity to amyloid β peptides linked to Alzheimer's disease and are suggested to be a potential therapeutic target [6, 7].

The α7 nAChR is one of the most abundant subtypes in the brain [8]. It is known to be expressed mainly in neurons [9], glial cells [10] not exclusively but predominantly in brain regions responsible for memory and learning [11, 12], and immune cells [13–16]. In addition to their role in synaptic transmission, α7 nAChRs also contribute to synaptic

Abbreviations: CHRNA7, the alpha7 nicotinic acetylcholine receptor; DAVID, The Database for Annotation, Visualization and Integrated Discovery; DDA, data dependent acquisition; KEEG, Kyoto Encyclopedia of Genes and Genomes; KO, knockout; RSLC, rapid separation liquid chromatography; WT, wild type.

plasticity [17], and in the periphery they are linked to the cholinergic anti-inflammatory pathway [18]. In the cerebellum, α7 nAChRs are expressed on the membranes of granule cells [19], which play a crucial role in regulating information flow within the cerebellar circuitry [20]. Moreover, α7 nAChRs are expressed in Purkinje cells and were reported to control the release of other transmitters such as GABA (γ-aminobutyric acid) or glutamate [21, 22]. Another study showed that α7 nAChR expression increases in developing rat cerebellum during important synapse growth stages [21, 23]. However, further specific roles of α7 nAChR in cerebellum are largely unknown and studies addressing consequences of CHRNA7 knockout (KO) at the proteome level are missing. Therefore, we conducted proteome analyses of the cerebellum from CHRNA7 KO mice. To verify to what extent α7 nAChR deficiency also affects organs without α7 nAChR-expression, we additionally analyzed liver samples from the same animals.

A KO mouse model was generated by deleting the last three exons (8–10) of the gene and was initially characterized by Orr-Urteger et al. and Paylor et al. [24, 25]. Using brain tissue from α7 nAChR-deficient mice and corresponding WT mice a previous proteomics study addressed the α7 nAChR interactome by affinity immobilization combined with mass spectrometry [26]. A further proteomics study addressed the function of α7 nAChR in the ovary was previously performed by Seßenhausen, Caban et al. [2]. Cerebellum and liver samples, analyzed in this study, stem from the same animals.

In brief, homozygote breeders for the α7 KO mouse strain on the B6. 129S7-Chrna7, (stock No. 0032327Acr7-) and age-matched wild-type C57Bl/6J mice (stock no. 000664) were purchased from Jackson Laboratory (Bar Harbor, ME, USA), and upon arrival young females were housed at the animal core facility at the BMC (Biomedical Center) until they reached the age of 3 months. The housing of laboratory mice followed European and German animal welfare laws. The experiment adhered to Section 4 of the German Animal Welfare Act. CHRNA7 KO mice ($n = 5$) and corresponding wild type (WT) female mice ($n = 5$), all in same cycle (metestrus), were sacrificed by cervical dislocation, and cerebella and livers were dissected. For protein extraction, 100 μL of 8 M of urea in 50 mM ammonium bicarbonate was added to approximately 1 mg of tissue. For cell lysis each sample was sonicated for 15 min by Bandelin Sonoplus HD3200 cup resonator (Bandelin, Berlin, Germany). For further homogenization, samples were centrifuged through QIAshredder devices (QIAGEN, Hilden, Germany) for 3 min (10°C, 2500×g). The Pierce 660 nm assay (Thermo Scientific, Waltham, MA, USA) was used to determine protein concentration [27]. Finally, 10 μg of protein was reduced at a concentration of 5 mM dithiothreitol, alkylated at a concentration of 15 mM iodoacetamide and quenched with 15 mM dithiothreitol for 15 min at room temperature in the dark. Digestion was performed with Lys-C (1:100, enzyme:protein-ratio, Wako, Osaka, Japan) for 4 h. Prior to the second digestion step, samples were diluted with 50 mM ammonium bicarbonate to obtain 1 M Urea. Trypsin was added (1:50, enzyme:protein-ratio, Promega) and incubated for 16 h at 37°C. For LC-MS/MS analysis, 1.5 μg of peptides aliquots were injected into an Ultimate 3000 RSLC chromatography system and transferred to a trap column (PEP-Map100 C18, 75 μm × 2 cm, 3 μm particles (Thermo Fisher Scientific, USA)) at a flow rate of 5 μL/min mobile phase A (0.1% formic acid and 1% acetonitrile in water). Separation was performed on a reversed-phase column (PepMap RSLC C18, 75 μm × 50 cm, 2 μm particles, Thermo Scientific, U.S.A) with a flow rate of 250 nL/min. The chromatographic method used a two-step gradient from 3% mobile phase of B phase (0.1% formic acid in acetonitrile) to 25% B in 160 min and a 10 min ramp to 40% B (A: 0.1% formic acid in water). MS analysis was performed with a Q Exactive HF-X (Thermo Scientific, Waltham, MA, USA) with a maximum of 15 MS/MS scans per cycle in the data-dependent acquisition mode. Mass spectra were acquired using a normalized collision energy of 27, resolution of 15 K, maximum inject time of 50 ms, and an automatic gain control (AGC) target of 1e6. The precursor range was set to $m/z = 350–1600$. For protein identification and label-free quantification, MaxQuant (2.3.0) [28] was used in combination with the *Mus musculus* subset of the UniProt database. The mass spectrometry proteomics data have been deposited to the ProteomeXchange Consortium via the PRIDE partner repository [29] with the project accession: PXD045358. Applying the above-mentioned workflow, we were able to identify 26,794 unique peptides and 29,769 peptides from the cerebellum KO and WT samples, which resulted in 3535 proteins (FDR < 0.01) 25,764 unique peptides and 23,898 peptides from liver KO and WT samples, which resulted in 2820 proteins (FDR < 0.01) (Table S1).

Data analysis was performed with Perseus (1.6.13.0) [30] and R together with the tidyverse (4.1.2) and enhanced volcano plot packages [31]. To ensure robust statistics, the hits of identified proteins were filtered for at least 70% valid quantitative values among KO or WT samples. To handle missing values the imputation feature implemented in Perseus was used. Significantly altered proteins were detected using a two-sample Student's *t*-test with a significance cut-off (s0 = 0.1, FDR < 0.05). Corresponding Volcano plot and bubble plots were performed in R (4.2.0).

The analysis of the liver tissue samples revealed no prominent proteomic alterations, with only three proteins more abundant in KOs (Table S2). However, in contrast 110 differentially abundant proteins (Log_2 FC > 0.6; q-value < 0.05) in mouse cerebellar samples were detected, of which 20 were less abundant and 90 were more abundant in the KO genotype. Table 1 displays the top 20 proteins altered in abundance in KO versus WT cerebella. Furthermore, the volcano plot (Figure 1A) depicts proteins which are altered in abundance in the CHRNA7 knockout compared to the WT proteomes of cerebellar samples (FDR < 0.05). Strikingly, GSN (Gelsolin) and IDE (Insulin degrading enzyme), known α7 nAChR interactors [32], were found among the proteins significantly altered in abundance. For downstream bioinformatics analysis DAVID was used [33].

DAVID analysis was used with the following categories: GO molecular function, GO biological process, Reactome, KEEG. Medium stringency was applied and resulted clusters were labeled according to the term with Enrichment Score > 1.3 and *p*-value < 0.05. The obtained results from the 110 differentially abundant proteins were then plotted in R. For the more abundant proteins (Figure 1B), five significantly enriched clusters were detected. The highest enrichment score showed the cluster "Glutamatergic synapse" and consists of GNG13, ITPR1, SLC38A1, SLC1A3, SLC17A7, SLC38A3, SLC1A6, SHANK1, SHANK2 (Figure 1C). A list of the corresponding proteins,

TABLE 1 List of top 20 proteins altered in abundance in CHRNA7 KO versus WT cerebellum.

Differentially abundant proteins in cellular proteomes					
Uniprot accession	Gene names	Protein names	Log_2FC	q-value	GO biological process (Uniprot)
More abundant in cellular proteomes					
P11881	Itpr1	Inositol 1,4,5-trisphosphate receptor type 1	3.61	0.042	Calcium transport
Q78PY7	Snd1	Staphylococcal nuclease domain-containing protein 1	3.52	0.037	Transcription regulation
P43276	Hist1h1b	Histone H1.5	3.24	0.037	Chromatin organization
P63158	Hmgb1	High mobility group protein B1	3.02	0.044	Adaptive immunity
Q64444	Ca4	Carbonic anhydrase 4	2.72	0.043	Bicarbonate transport
Q9D1L0	Chchd2	Coiled-coil-helix-coiled-coil-helix domain-containing protein 2	2.71	0	Transcription
O35544	Slc1a6	Excitatory amino acid transporter 4	2.62	0.035	Amino-acid transport
Q2PFD7	Psd3	PH and SEC7 domain-containing protein 3	2.57	0.006	ARF protein signal transduction
P43275	Hist1h1a	Histone H1.1	2.56	0.037	DNA binding
Q61029	Tmpo	Lamina-associated polypeptide 2, isoforms beta/delta/epsilon/gamma	2.53	0.035	regulation of DNA-templated transcription
Less Abundant in cellular proteomes					
Q5EBJ4	Ermn	Ermin	−2.63	0.04	actin filament organization
O08997	Atox1	Copper transport protein ATOX1	−2.40	0.03	Ion transport
Q9D2P8	Mobp	Myelin-associated oligodendrocyte basic protein	−2.23	0.04	central nervous system myelin formation
P62482	Kcnab2	Voltage-gated potassium channel subunit beta-2	−2.08	0.04	Ion transport
Q61885	Mog	Myelin-oligodendrocyte glycoprotein	−1.97	0.04	regulation of cytokine production
P13020	Gsn	Gelsolin	−1.96	0.04	Cilium biogenesis/degradation
O70172	Pip4k2a	Phosphatidylinositol 5-phosphate 4-kinase type-2 alpha	−1.85	0.04	Lipid matabolism
Q8VDQ8	Sirt2	NAD-dependent protein deacetylase sirtuin-2	−1.67	0.04	autophagy
Q80W21	Gstm7	Glutathione S-transferase Mu 7	−1.51	0	glutathione metabolic process
Q62188	Dpysl3	Dihydropyrimidinase-related protein 3	−1.37	0.04	nervous system development

including the Log2 FC, q, and iBAQ values, can be found in Table 2. Interestingly, 28 other proteins (Table S3) related to a glutamatergic synapse pathway were identified which did not reach statistical significance (FDR < 0.05) in the Student's *t*-test (KO vs. WT).

Our results, therefore, suggest that the absence of these receptors could trigger changes in glutamatergic signaling to compensate for the loss of cholinergic input. Studies from glutamatergic synaptic transmission showed that presynaptic α7 nAChRs mediate enhancement of glutamate release. That could activate calcium-dependent signaling cascades [34], which might further contribute to the significance of proteins related to the glutamatergic pathway in the absence of a7 nicotinic receptors. Additionally, the absence of α7 nicotinic receptors raises the possibility of alterations in acetylcholine release, which might lead to subsequent changes in the release of glutamate. Nevertheless, further research is needed to investigate the extent of this potential influence.

Among the less abundant proteins, the DAVID analysis displayed two significantly enriched clusters. While the most enriched cluster was the rather general term "cytosol," the term "myelin sheath" was the second most significant cluster which comprised: GSN, MOG, MOBP, TPPP, ERMN, SIRT2. A list of the corresponding proteins, including the Log2 FC, q and iBAQ values, can be found in Table 2. So far the α7 nicotinic receptor was not described to be directly involved in the formation and maintenance of the myelin sheath. The myelin sheath is produced by oligodendrocytes in the central nervous system and is a crucial component of the nervous system as it insulates and protects nerve fibers, allowing for efficient transmission of electrical impulses [35]. Interestingly, Scott W. Rogers et al. detected transcripts of α7 nAChR in oligodendrocyte precursor cells (OPCs), a subtype of glial cells responsible for myelin regeneration (oligodendrocytes originate from OPCs) [36]. Among the less abundant proteins associated with the myelin sheath, we found gelsolin (GSN) which is an actin-modulating protein that is calcium regulated and plays a role in nucleation and apoptotic processes [37] and sirtuin 2 (SIRT2) which is involved in the regulation of lysosome mediated degradation of protein aggregates by autophagy in neuronal cells [38].

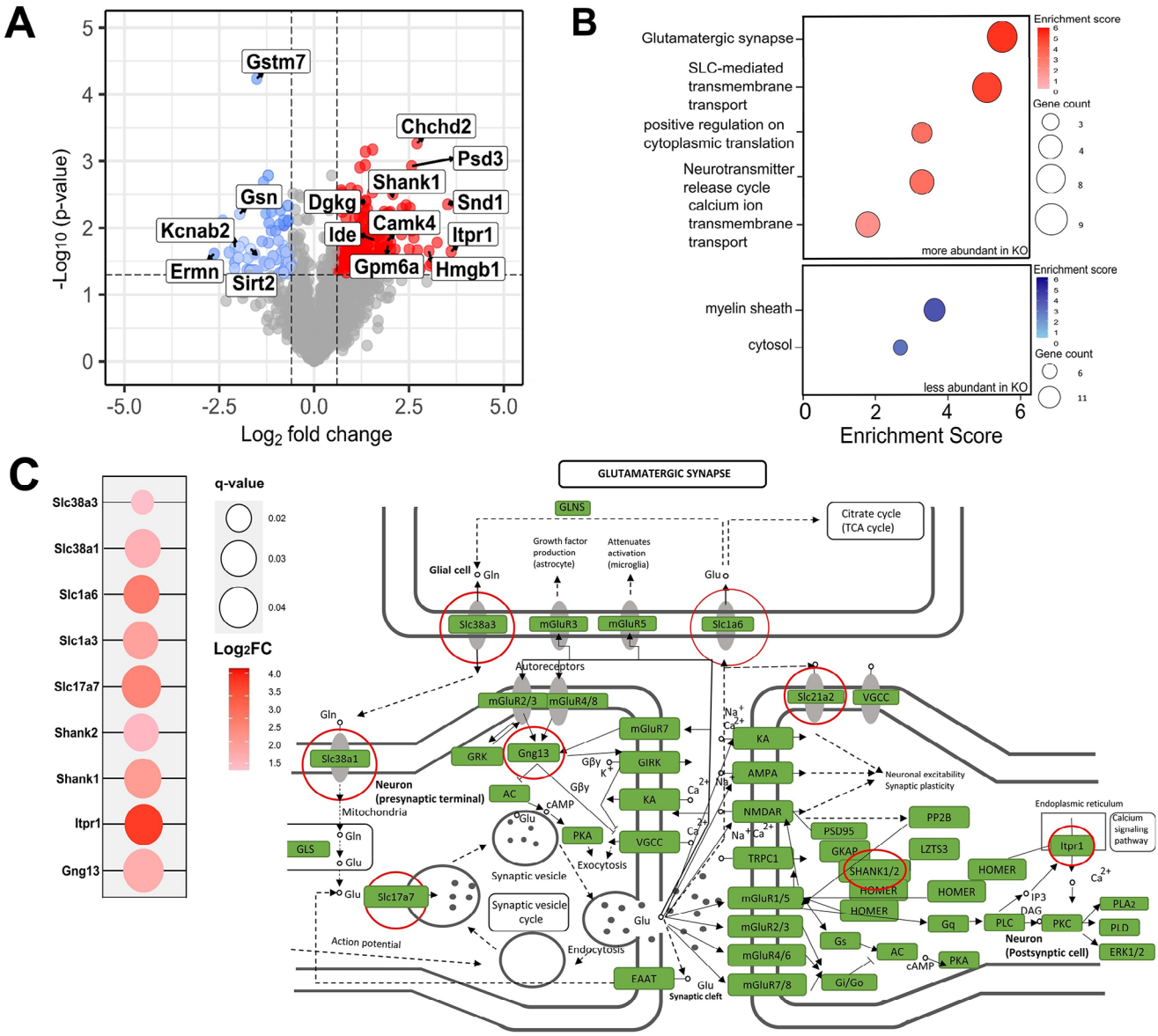

FIGURE 1 (A) Volcano plot of cerebellum protein intensity values in KO versus WT samples. Significantly altered proteins were detected with nonpaired t-test with false discovery rate (FDR) correction (0.05). Each colored dot represents a protein fulfilling the significance criteria (|Log2 FC| > 0.6; *p*-value < 0.05). (B) Bubble plot of functionally enriched GO terms with Enrichment Scores > 1.3 and *p*-values < 0.05 of proteins more and less abundant in KO cerebellum samples. The enriched clusters are represented by the GO term and are categorized based on molecular function, biological process KEGG pathway and Reactome pathway. (C) Glutamatergic synapse-KEEG pathway. Labeled proteins are those with higher abundance in the knockout (KO) mice. Abundance alterations are color coded and shown as Log2FC. Circle size correlates with q-value.

We also found decreased levels of the myelin-oligodendrocyte glycoprotein (MOG), which is a glycoprotein essential in the myelination of nerves in the central nervous system (CNS). Moreover, this protein is an important component of the oligodendrocyte surface membranes and has, together with others, fundamental roles in the formation, maintenance and disintegration of myelin sheaths [39, 40]. Likewise, we found the myelin-associated oligodendrocyte basic protein (MOBP) as one of the most decreased proteins in KO cerebellum samples. Strikingly, MOBP is a structural constituent of myelin sheath, shares several characteristics with MBP protein and is associated with multiple sclerosis (MS) [41]. We further detected decreased ermin (ERMN) levels in KO cerebellum samples, a protein which plays a role in cytoskeletal rearrangement during the compaction phase of myelinogenesis as well as in the maintenance and stability of myelin sheath [42]. Taken together, it can be speculated that the deletion of CHRNA7 affects myelin sheath and, consequently, the efficiency of neural communication and processing in the cerebellum. However, the specific involvement of CHRNA7 remains to be shown.

In conclusion, our dataset demonstrates that the deletion of CHRNA7 has significant effects on the proteome of the cerebellum, particularly with regards to myelin sheath formation, ion transport and glutamatergic synapses. Although a proteomic dataset does not allow to fully elucidate the impact of CHRNA7 on this part of the nervous system, the dataset gives new insights and could be the basis for

TABLE 2 List of proteins altered in abundance in CHRNA7 KO in "Glutamatergic synapse" and decreased in abundance in CHRNA7 KO in "Myelin Sheath.

Uniprot accession	Gene names	Protein names	Log_2 FC	q-value	iBAQ values	
					iBAQ WT	iBAQ KO
GLUTAMATERGIC SYNAPSE						
P11881	Itpr1	Inositol 1,4,5-trisphosphate receptor type 1	3.61	0.04	2.62E+07	2.09E+08
O35544	Slc1a6	Excitatory amino acid transporter 4	2.63	0.00	1.64E+07	1.61E+08
Q3TXX4	Slc17a7	Vesicular glutamate transporter 1	2.48	0.05	5.88E+06	4.52E+07
D3YZU1	Shank1	SH3 and multiple ankyrin repeat domains protein 1	2.07	0.04	1.96E+06	2.77E+07
P56564	Slc1a3	Excitatory amino acid transporter 1	1.96	0.03	1.16E+08	7.39E+08
Q9JMF3	Gng13	Guanine nucleotide-binding protein G(I)/G(S)/G(O) subunit gamma-13	1.73	0.05	1.15E+07	6.78E+07
Q8K2P7	Slc38a1	Sodium-coupled neutral amino acid transporter 1	1.63	0.04	8.83E+05	1.02E+07
Q80Z38	Shank2	SH3 and multiple ankyrin repeat domains protein 2	1.47	0.03	4.09E+05	6.38E+06
Q8K2P7	Slc38a3	Sodium-coupled neutral amino acid transporter 3	1.35	0.02	2.71E+06	1.12E+07
MYELIN SHEATH						
Q5EBJ4	Ermn	Ermin	−2.64	0.05	8.68E+07	2.50E+07
Q9D2P8	Mobp	Myelin-associated oligodendrocyte basic protein	−2.24	0.05	1.59E+08	6.52E+07
Q61885	Mog	Myelin-oligodendrocyte glycoprotein	−1.97	0.04	9.91E+08	3.35E+08
P13020	Gsn	Gelsolin	−1.96	0.04	1.59E+08	6.52E+07
Q8VDQ8	Sirt2	NAD-dependent protein deacetylase sirtuin-2	−1.68	0.05	4.04E+08	1.24E+08
Q7TQD2	Tppp	Tubulin polymerization-promoting protein	−1.12	0.04	9.91E+08	3.35E+08

further investigations addressing the localization and functional roles of α7 nAChR in the cerebellum.

ACKNOWLEDGMENTS

This study was funded by the Deutsche Forschungsgemeinschaft–Project number-432434245 (to Thomas Fröhlich and Artur Mayerhofer).

Open access funding enabled and organized by Projekt DEAL.

CONFLICT OF INTEREST STATEMENT

The authors declare no conflict of interest.

DATA AVAILABILITY STATEMENT

The mass spectrometry proteomics data have been deposited to the PRIDE repository, dataset identifier PXD045358.

ORCID

Thomas Fröhlich https://orcid.org/0000-0002-4709-3211

REFERENCES

1. Unwin, N. (2005). Refined structure of the nicotinic acetylcholine receptor at 4Å resolution. *Journal of Molecular Biology*, *346*(4), 967–989.
2. Seßenhausen, P., Caban, K. M., Kreitmair, N., Peitzsch, M., Stöckl, J. B., Pépin, D., Popper, B., Fröhlich, T., & Mayerhofer, A. (2023). An ovarian phenotype of alpha 7 nicotinic receptor knock out mice. *Reproduction*, *166*(3), 221–234.
3. Dani, J. A., & Bertrand, D. (2007). Nicotinic acetylcholine receptors and nicotinic cholinergic mechanisms of the central nervous system. *Annual Review of Pharmacology and Toxicology*, *47*, 699–729.
4. Weng, P.-H., Chen, J.-H., Chen, T.-F., Sun, Y., Wen, L.-L., Yip, P.-K., Chu, Y.-M, & Chen, Y.-C. (2016). CHRNA7 polymorphisms and dementia risk: Interactions with apolipoprotein ε4 and cigarette smoking. *Scientific Reports*, *6*(1), 27231.
5. Corringer, P.-J., Bertrand, S., Galzi, J.-L., Devillers-Thiéry, A., Changeux, J.-P., & Bertrand, D. (1999). Mutational analysis of the charge selectivity filter of the α7 nicotinic acetylcholine receptor. *Neuron*, *22*(4), 831–843.
6. Wu, J., Liu, Q., Tang, P., Mikkelsen, J. D., Shen, J., Whiteaker, P., & Yakel, J. L. (2016). Heteromeric $\alpha7\beta2$ nicotinic acetylcholine receptors in the brain. *Trends in Pharmacological Sciences*, *37*(7), 562–574.
7. Whiteaker, P., & George, A. A. (2023). Discoveries and future significance of research into amyloid-beta/α7-containing nicotinic acetylcholine receptor (nAChR) interactions. *Pharmacological Research*, *191*, 106743.
8. Dani, J. A. (2015). Neuronal nicotinic acetylcholine receptor structure and function and response to nicotine. *International Review of Neurobiology*, *124*, 3–19.
9. Dineley, K T., Pandya, A A., & Yakel, J. L. (2015). Nicotinic ACh receptors as therapeutic targets in CNS disorders. *Trends in Pharmacological Sciences*, *36*(2), 96–108.

10. Agulhon, C., Petravicz, J., Mcmullen, A B., Sweger, E. J., Minton, S. K., Taves, S. R., Casper, K. B., Fiacco, T. A., & Mccarthy, K. D. (2008). What is the role of astrocyte calcium in neurophysiology? *Neuron*, *59*(6), 932–946.
11. Levin, E. D. (2012). α7-nicotinic receptors and cognition. *Current Drug Targets*, *13*(5), 602–606.
12. Leiser, S. C., Bowlby, M. R., Comery, T. A., & Dunlop, J. (2009). A cog in cognition: How the α7 nicotinic acetylcholine receptor is geared towards improving cognitive deficits. *Pharmacology & Therapeutics*, *122*(3), 302–311.
13. Wang, H., Yu, M., Ochani, M., Amella, C. A., Tanovic, M., Susarla, S., Li, J. H., Wang, H., Yang, H., Ulloa, L., Al-Abed, Y., Czura, C. J., & Tracey, K. J. (2003). Nicotinic acetylcholine receptor α7 subunit is an essential regulator of inflammation. *Nature*, *421*(6921), 384–388.
14. Wessler, I., & Kirkpatrick, C. J. (2008). Acetylcholine beyond neurons: the non-neuronal cholinergic system in humans. *British Journal of Pharmacology*, *154*(8), 1558–1571.
15. Shen, J.-X., & Yakel, J. L. (2012). Functional α7 nicotinic ACh receptors on astrocytes in rat hippocampal CA1 slices. *Journal of Molecular Neuroscience*, *48*(1), 14–21.
16. Sharma, G., & Vijayaraghavan, S. (2001). Nicotinic cholinergic signaling in hippocampal astrocytes involves calcium-induced calcium release from intracellular stores. *Proceedings of the National Academy of Sciences USA*, *98*, 4148–4153.
17. Xu, Z.-Q., Zhang, W.-J., Su, D.-F., Zhang, G.-Q., & Miao, C-Y. (2021). Cellular responses and functions of α7 nicotinic acetylcholine receptor activation in the brain: a narrative review. *Annals of Translational Medicine*, *9*(6), 509.
18. Wu, Y.-J, Wang, L., Ji, C.-F., Gu, S.-F., Yin, Q., & Zuo, J. (2021). The role of α7nAChR-mediated cholinergic anti-inflammatory pathway in immune cells. *Inflammation*, *44*(3), 821–834.
19. Caruncho, H. J., Guidotti, A., Lindstrom, J., Costa, E., & Pesold, C. (1997). Subcellular localization of the α7 nicotinic receptor in rat cerebellar granule cell layer. *Neuroreport*, *8*(6), 1431–1433.
20. Goldowitz, D. (1998). The cells and molecules that make a cerebellum. *Trends in Neurosciences*, *21*(9), 375–382.
21. Lee, M. (2002). Nicotinic receptor abnormalities in the cerebellar cortex in autism. *Brain*, *125*(7), 1483–1495.
22. Encyklopaedia, T. E. o. (2015). "Purkinje cell", in Encyclopedia Britannica.
23. De Toro, E. D., Juíz, J. M., Smillie, F. I., Lindstrom, J., & Criado, M. (1997). Expression of α 7 neuronal nicotinic receptors during postnatal development of the rat cerebellum. *Brain Research Developmental Brain Research*, *98*(1), 125–133.
24. Orr-Urtreger, A., Göldner, F. M., Saeki, M., Lorenzo, I., Goldberg, L., De Biasi, M., Dani, J. A., Patrick, J. W., & Beaudet, A. L. (1997). Mice deficient in the α7 neuronal nicotinic acetylcholine receptor lack α-bungarotoxin binding sites and hippocampal fast nicotinic currents. *The Journal of Neuroscience*, *17*(23), 9165–9171.
25. Paylor, R., Nguyen, M., Crawley, J. N., Patrick, J., Beaudet, A., & Orr-Urtreger, A. (1998). α7 nicotinic receptor subunits are not necessary for hippocampal-dependent learning or sensorimotor gating: A behavioral characterization of Acra7-deficient mice. *Learning & Memory (Cold Spring Harbor, N.Y.)*, *5*(4-5), 302–316.
26. Paulo, J. A., Brucker, W. J., & Hawrot, E. (2009). Proteomic analysis of an α7 nicotinic acetylcholine receptor interactome. *Journal of Proteome Research*, *8*(4), 1849–1858.
27. Bradford, M. M. (1976). A rapid and sensitive method for the quantitation of microgram quantities of protein utilizing the principle of protein-dye binding. *Analytical Biochemistry*, *72*, 248–254.
28. Cox, J., Hein, M. Y., Luber, C. A., Paron, I., Nagaraj, N., & Mann, M. (2014). Accurate proteome-wide label-free quantification by delayed normalization and maximal peptide ratio extraction, Termed MaxLFQ*. *Molecular & Cellular Proteomics*, *13*(9), 2513–2526.
29. Perez-Riverol, Y., Csordas, A., Bai, J., Bernal-Llinares, M., Hewapathirana, S., Kundu, D. J., Inuganti, A., Griss, J., Mayer, G., Eisenacher, M., Pérez, E., Uszkoreit, J., Pfeuffer, J., Sachsenberg, T., Yilmaz, S., Tiwary, S., Cox, J., Audain, E., Walzer, M., … Vizcaíno, J. A. (2018). The PRIDE database and related tools and resources in 2019: improving support for quantification data. *Nucleic Acids Research*, *47*(D1), D442–D450.
30. Tyanova, S., Temu, T., Sinitcyn, P., Carlson, A., Hein, M. Y., Geiger, T., Mann, M., & Cox, J. (2016). The Perseus computational platform for comprehensive analysis of (prote)omics data. *Nature Methods*, *13*(9), 731–740.
31. Blighe, K. R. S., & Lewis, M. (2022). *Publication-ready volcano plots with enhanced colouring and labeling*. github.
32. Mulcahy, M. J., Paulo, J. A., & Hawrot, E. (2018). Proteomic investigation of murine neuronal α7-nicotinic acetylcholine receptor interacting proteins. *Journal of Proteome Research*, *17*(11), 3959–3975.
33. Huang, Da. W, Sherman, B. T., & Lempicki, R. A. (2008). Bioinformatics enrichment tools: Paths toward the comprehensive functional analysis of large gene lists. *Nucleic Acids Research*, *37*(1), 1–13.
34. Cheng, Q., & Yakel, J L. (2015). The effect of α7 nicotinic receptor activation on glutamatergic transmission in the hippocampus. *Biochemical Pharmacology*, *97*(4), 439–444.
35. Susuki, K. (2010). Myelin: A specialized membrane for cell communication. *Nature Education*, *3*(9), 59.
36. Rogers, S. W., Gregori, N. Z., Carlson, N., Gahring, L. C., & Noble, M. (2001). Neuronal nicotinic acetylcholine receptor expression by O2A/oligodendrocyte progenitor cells. *Glia*, *33*(4), 306–313.
37. Yin, H. L. (1987). Gelsolin: Calcium- and polyphosphoinositide-regulated actin- modulating protein. *BioEssays*, *7*(4), 176–179.
38. Gal, J., Bang, Y., & Choi, H. J. (2012). SIRT2 interferes with autophagy-mediated degradation of protein aggregates in neuronal cells under proteasome inhibition. *Neurochemistry International*, *61*(7), 992–1000.
39. Quarles, R. H. (2002). Myelin sheaths: glycoproteins involved in their formation, maintenance and degeneration. *Cellular and Molecular Life Sciences*, *59*(11), 1851–1871.
40. Ambrosius, W., Michalak, S., Kozubski, W., & Kalinowska, A. (2020). Myelin oligodendrocyte glycoprotein antibody-associated disease: Current insights into the disease pathophysiology, diagnosis and management. *International Journal of Molecular Sciences*, *22*(1), 100.
41. Yoshikawa, H. (2001). Myelin-associated oligodendrocytic basic protein modulates the arrangement of radial growth of the axon and the radial component of myelin. *Medical Electron Microscopy*, *34*(3), 160–164.
42. Brockschnieder, D., Sabanay, H., Riethmacher, D., & Peles, E. (2006). Ermin, a myelinating oligodendrocyte-specific protein that regulates cell morphology. *The Journal of Neuroscience*, *26*(3), 757.

SUPPORTING INFORMATION

Additional supporting information may be found online https://doi.org/10.1002/pmic.202300384 in the Supporting Information section at the end of the article.

How to cite this article: Caban, K. M., Seßenhausen, P., Stöckl, J. B., Popper, B., Mayerhofer, A., & Fröhlich, T. (2024). Proteome profile of the cerebellum from α7 nicotinic acetylcholine receptor deficient mice. *Proteomics*, e2300384. https://doi.org/10.1002/pmic.202300384